the approach, however, necessitates the development of engineering correlations for C_M and C_H. Such correlations have been developed for graphite ablation in air and are presented in Ref. 6. Correlations for additional materials are in progress. Results to date suggest that C_M approaches C_H when the system Lewis number (as defined in Ref. 1) approaches unity, but that the conventional relation [$C_M/C_H = (\mathrm{Le})^{2/3}$] can be in substantial error for large mass-transfer rates, especially when the injectant reacts chemically with the edge gases.[5] Such correlations will eventually provide a means for rapidly and accurately predicting unequal-diffusion ablation response from relatively well-known nonablating heat-transfer coefficients.

References

[1] Kendall, R. M., Rindal, R. A., and Bartlett, E. P., "A Multicomponent Boundary Layer Chemically Coupled to an Ablating Surface," *AIAA Journal*, Vol. 5, No. 6, June 1967, pp. 1063–1071.

[2] Kendall, R. M. and Bartlett, E. P., "Nonsimilar Solution of the Multicomponent Laminar Boundary Layer by an Integral-Matrix Method," *AIAA Journal*, Vol. 6, No. 6, June 1968, pp. 1089–1097.

[3] Kendall, R. M. and Rindal, R. A., "Analytical Evaluation of Rocket Nozzle Ablation," AIAA Paper 64-101, Palo Alto, Calif., 1964.

[4] Kendall, R. M., "An Analysis of the Coupled Chemically Reacting Boundary Layer and Charring Ablator—Part V, A General Approach to the Thermochemical Solution of Mixed Equilibrium-Nonequilibrium, Homogeneous or Heterogeneous Systems," NASA CR-1064, June 1968, Aerotherm Corp., Mountain View, Calif.

[5] Bartlett, E. P. and Grose, R. D., "An Evaluation of a Transfer Coefficient Approach for Unequal Diffusion Coefficients," Sandia Rept. SC-CR-69-3270, June 1969, Aerotherm Corp., Mountain View, Calif.

[6] Bartlett, E. P. and Grose, R. D., "The Multicomponent Laminar Boundary Layer Over Graphite Sphere Cones: Solutions for Quasisteady Ablation and Application to Transient Reentry Trajectories," Sandia Rept. SC-CR-68-3665, May 1968, Aerotherm Corp., Mountain View, Calif.

Velocity Laws for Turbulent Boundary Layers with Mass Addition and Combustion

L. K. Isaacson* and J. W. Jones†

University of Utah, Salt Lake City, Utah

THIS Note presents the results of a study directed toward the use of the turbulent kinetic energy equation as the basic closure equation for the problem of a subsonic variable density turbulent boundary layer. The case considered is that of a uniform two-dimensional, turbulent boundary layer with a dilute mixture of hydrogen and nitrogen injected into the boundary layer at the surface and combustion occurring at a flame front in the boundary layer. The method of analysis presented is an extension of the methods employed by Townsend,[1] Bradshaw, et al.,[2] Bradshaw,[3] and Bradshaw and Ferriss.[4]

Received October 20, 1969; revision received February 24, 1970. Supported by the U.S. Air Force Office of Scientific Research under Project THEMIS, Contract No. F44620-68-C-0022.

* Associate Professor, Department of Mechanical Engineering. Member AIAA.

† NASA Trainee, Department of Mechanical Engineering; presently post-doctoral fellow at The Ohio State University, Columbus, Ohio. Member AIAA.

The turbulent kinetic energy equation is utilized to obtain expressions for the velocity distribution through the boundary layer for the case of a zero axial pressure gradient. Similarity between the concentration, enthalpy, and velocity profiles is employed in order to relate the local density to the local velocity. Experimental results are correlated on the basis of the resulting expressions over the inner region of the turbulent boundary layer. These correlations indicate the energy dissipation length is directly proportional to distance from the surface over approximately 10% of the boundary-layer thickness at the higher blowing rates.

The turbulent kinetic energy equation for a two-dimensional compressible flow may be written as [1,2]

$$\langle\rho\rangle\langle U\rangle\partial\langle q^2/2\rangle/\partial x + \langle\rho\rangle\langle V\rangle\partial\langle q^2/2\rangle/\partial y + \langle\rho uv\rangle\,\partial\langle U\rangle/\partial y + \partial(\langle pv\rangle + \langle\rho q^2 v/2\rangle)/\partial y + \langle\rho\rangle\epsilon = 0 \quad (1)$$

where $\langle U\rangle$ and $\langle V\rangle$ are the mean velocities in the x and y directions, respectively, $\langle q^2\rangle = \langle u^2\rangle + \langle v^2\rangle + \langle w^2\rangle$, p is the pressure fluctuation, $\langle\rho\rangle$ is the mean density, u, v, and w are the velocity fluctuations and ϵ is the dissipation of turbulent kinetic energy due to viscous effects. Equation (1) represents the rate of change of $\langle q^2/2\rangle$ along a streamline as the net sum of advection, production, diffusion, and viscous dissipation of the turbulent kinetic energy.

The turbulent kinetic energy equation may be converted into a shear stress equation by defining[1,2]

$$\tau/\langle\rho\rangle = -\langle\rho uv\rangle/\langle\rho\rangle \quad (2a)$$

$$a_1 = \tau/(\langle\rho\rangle\langle q^2\rangle) \quad (2b)$$

$$L = (\tau/\langle\rho\rangle)^{3/2}/\epsilon \quad (2c)$$

and

$$(1/\langle\rho\rangle)\partial(\langle pv\rangle + \langle\rho q^2 v/2\rangle)/\partial y = a_2\partial(\langle q^2\rangle)^{3/2}/\partial y \quad (2d)$$

In Eqs. (2) τ is the local shear stress, L is an energy dissipation length, and a_1 and a_2 are constants. The hypothesis of turbulence structural equilibrium as employed by Townsend[1] is used to justify the form of the diffusion term chosen in Eq. (2d).

Thus, for the case of surface mass injection with combustion, we may write, neglecting the variation of $\langle q^2/2\rangle$ in the x direction and setting $V = V_w$,

$$[1/(\tau/\rho)^{1/2}]dU - 1/(2\tau/\rho)d(\tau/\rho) - (V_w/2a_1)[1/(\tau/\rho)^{3/2}]d(\tau/\rho) = (1/L)dy \quad (3)$$

where all brackets denoting average quantities have been dropped.

In obtaining this expression, the factor $3a_2/2(a_1)^{3/2}$ has been set equal to $\frac{1}{2}$, following the arguments of Townsend.[1] It should also be noted that the approximation of $V = V_w$ was found to be necessary in order to achieve the correlations presented. When V is set equal to $(\rho_w/\rho)V_w$, the advection term becomes dominant due to the significant decrease in the density ρ across the inner region of the boundary layer and correlation of the velocity profile with distance from the surface is not achieved. The successful correlation achieved with setting $V = V_w$ may possibly be explained by noting that very near the surface, the effect on the density of the increasing temperature is offset somewhat by the effect of the decreasing concentration of hydrogen and the approximation $V = V_w$ appears to be sufficiently accurate. With V set equal to V_w, the contribution of the advection term is suppressed in the region away from the immediate vicinity of the wall and the production and dissipation terms in the kinetic energy equation become the dominant terms.

For the turbulent boundary layer with mass addition and zero pressure gradient, the mean momentum equation may be written as

$$\tau/\rho = (\rho_w/\rho)(\tau_w/\rho_w + V_w U) \quad (4)$$

With the introduction of the friction velocity, $u_\tau = (\tau_w/\rho_w)^{1/2}$, Eq. (4) may be written as

$$\tau/\rho = (\rho_w/\rho)(u_\tau^2)[1 + (V_w/u_\tau)u^+] \quad (5)$$

where $u^+ = U/u_\tau$. Substitution into Eq. (3) yields the result

$$[(\rho_w/\rho)\{1 + (V_w/u_\tau)u^+\}]^{-1/2}du^+ - (1/2)d\ln[(\rho_w/\rho)\{1 + (V_w/u_\tau)u^+\}] - (V_w/u_\tau 2a_1)[(\rho_w/\rho)\{1 + (V_w/u_\tau)u^+\}]^{-3/2} \times d[(\rho_w/\rho)(1 + \{V_w/u_\tau)u^+\}] = (1/L^+)dy^+ \quad (6)$$

where $y^+ = yu_\tau/\nu_w$ and $L^+ = Lu_\tau/\nu_w$.

To integrate the first term on the left-hand side of Eq. (6) (the production term), it is necessary to express the density ratio ρ_w/ρ in terms of the local velocity U. This is accomplished by assuming the flame sheet model as employed by Chen and Toong,[5] in their study of the laminar boundary layer with surface fuel evaporation and combustion.

The turbulent boundary layer is separated into two regions, region I, which lies between the wall and the flame zone, and region II, the region between the flame zone and the outer edge of the boundary layer. The presence of a discontinuous flame front within the boundary layer introduces discontinuities in the gradients of the mass fractions of the reactants and products and of the temperature in regions I and II of the boundary layer. However, as Chen and Toong[5] point out, when the production of the sensible enthalpy at any point in the boundary layer is set equal to the disappearance of the oxidizer times a constant heat of reaction, the profiles of mass fraction and temperature then become continuous throughout the boundary layer. Furthermore, the experimental results of Wooldridge and Muzzy[6] justify the use of similarity between concentration, enthalpy (including both sensible and chemical parts), and velocity profiles. Hence, we may write

$$h_c = h_{cw} + (h_{ce} - h_{cw})(U/U_e) \quad (7)$$

where

$$h_{ce} = c_{pe}T_e + QC_{0e} \quad (8)$$

$$h_{cw} = c_{pw}T_w \quad (9)$$

and

$$h_c = \begin{cases} c_pT \text{ in region I} \\ c_pT + QC_0 \text{ in region II} \end{cases} \quad (10)$$

In these expressions, h_c is the sensible plus chemical enthalpy, Q is the heat of combustion per unit mass of oxygen, and C_0 is the mass fraction of unburned oxygen in region II of the boundary layer. C_{0_e} is thus the mass fraction of oxygen in the freestream.

In order to obtain an expression for the variation of C_0 in the region between the flame front and the outer edge of the boundary layer, the expressions developed by Chen and Toong[5] are employed in the following fashion. First, the mass fraction is written as

$$C = C_0 - \alpha C_F \quad (11)$$

with

$$C = -\alpha C_F \text{ in region I} \quad (12)$$

and

$$C = C_0 \text{ in region II} \quad (13)$$

In these expressions, α is the stoichiometric ratio of the diffusion rates of oxygen and fuel at the flame front. Then, in region II, similarity between the mass fraction profile and the velocity profile yields the relationship

$$C_0 = C_w + (C_e - C_w)(U/U_e) \quad (14)$$

However, from Eq. (12), the mass fraction at the surface may be written as

$$C_w = -\alpha C_{F_w} \quad (15)$$

Hence, the mass fraction of unburned oxygen in region II of the boundary layer may be written as

$$C_0 = -\alpha C_{F_w} + (C_{0_e} + \alpha C_{F_w})(U/U_e) \quad (16)$$

In this expression, C_{F_w} is the mass fraction of fuel at the wall and the subscripts w and e denote evaluation of the particular quantity at the wall and at the edge of the boundary layer, respectively.

Thus, the density profile may be written for each of the two regions as follows.

Region I:

$$\rho_w/\rho = (T/T_w)(M_w/M) = (M_wC_{pw}/MC_p)\{1 + [(C_{pe}T_e/C_{pw}T_w) - 1 + (QC_{0e}/C_{pw}T_w)](u^+/u_e^+)\} \quad (17)$$

where $u_e^+ = U_e/u_\tau$ and M is the molecular weight.

Region II:

$$\rho_w/\rho = (T/T_w)(M_w/M) = (M_wC_{pw}/MC_p)\{1 + (QC_{0e}/C_{pw}T_w)(\alpha C_{F_w}/C_{0e}) + [(C_{pe}T_e/C_{pw}T_w) - 1 - (QC_{0e}/C_{pw}T_w)(\alpha C_{F_w}/C_{0e})](u^+/u_e^+)\} \quad (18)$$

At this point, we may note that the variation of the term (M_wC_{pw}/MC_p) across the boundary layer is small and, hence, the ratio may be taken as unity. We should also note that the experimental temperature profile for each corresponding velocity profile was used to obtain values for the heats of reaction QC_{0_e} and $Q\alpha C_{F_w}$ for use in Eqs. (17) and (18).

For convenience, we introduce the following terms

$$A_1 = [(C_{pe}T_e/C_{pw}T_w) - 1 + (QC_{0e}/C_{pw}T_w)](1/u_e^+) \quad (19)$$

$$A_2 = V_w/u_\tau \quad (20)$$

$$A_3 = 1 + (QC_{0e}/C_{pw}T_w)(\alpha C_{F_w}/C_{0e}) \quad (21)$$

$$A_4 = [(C_{pe}T_e/C_{pw}T_w)(1/A_3) - 1](1/u_e^+) \quad (22)$$

Hence, the shear stress equation for each of the two regions may be written as follows.

Region I:

$$[(1 + A_1u^+)(1 + A_1u^+)]^{-1/2}du^+ - \tfrac{1}{2}d\ln[(1 + A_1u^+)(1 + A_2u^+)] - (A_2/2a_1)[(1 + A_1u^+)(1 + A_2u^+)]^{-3/2} \times d[(1 + A_1u^+)(1 + A_2u^+)] = (1/L^+)dy^+ \quad (23)$$

Region II:

$$[A_3(1 + A_4u^+)(1 + A_2u^+)]^{-1/2}du^+ - \tfrac{1}{2}d\ln[A_3(1 + A_4u^+)(1 + A_2u^+)] - (A_2/2a_1)[A_3(1 + A_4u^+)(1 + A_2u^+)]^{-3/2} \times d[A_3(1 + A_4u^+)(1 + A_2u^+)] = (1/L^+)dy^+ \quad (24)$$

Integration of Eqs. (23) and (24) yields the result for the two regions as

Region I:

$$[2/(A_1A_2)^{1/2}]\ln[(A_2)^{1/2}(1 + A_1u^+)^{1/2} + (A_1)^{1/2} \times (1 + A_2u^+)^{1/2}] - \tfrac{1}{2}\ln[(1 + A_1u^+)(1 + A_2u^+)] + (A_2/a_1)[(1 + A_1u^+)(1 + A_2u^+)]^{-1/2} = \int(1/L^+)dy^+ + C_1 = F_I(u^+) \quad (25)$$

Table 1 Summary of experimental parameters for subsonic turbulent boundary layers with mass addition and combustion

Run	U_e, fps	$Re_x{}^c \times 10^{-5}$	$F^d \times 10^3$	$C_f{}^e \times 10^3$	T_w, °R	T_e, °R	C_{F_w}	QCo_e (exp)	$\alpha C_{Fw}/Co_e$ (exp)	A_1	A_2	A_3	A_4
WM1[a]	36	7.65	2.34	2.1	1032	573	0.04	968	2.33	0.0943	0.123	6.505	−0.0528
WM2	36	7.10	4.34	0.93	747	563	0.04	874	5.56	0.0794	0.294	17.793	−0.0308
WM3	36	6.32	7.56	0.28	625	573	0.04	764	13.69	0.0428	0.848	44.26	−0.0155
Jones1[b]	33.2	5.5	3.12	0.90	700	537	0.038	1068	1.50	0.106	0.208	7.233	−0.028
Jones2	33.6	6.4	3.12	0.89	640	545	0.038	1030	1.81	0.112	0.199	8.942	−0.0267
Jones3	33.5	7.1	3.12	0.85	640	544	0.038	929	2.07	0.0976	0.204	9.175	−0.0261

[a] See Wooldridge and Muzzy, Ref. 6.
[b] See Jones, Ref. 7.
[c] Reynolds' number based on distance from virtual origin $Re_x = \rho_e U e x/\mu_e$.
[d] Mass injection rate $F = \rho_w V_w/\rho_e U_e$.
[e] Skin-friction coefficient with mass injection and combustion $\tau_w = \frac{1}{2}\rho_e U_e{}^2 C_f$.

Region II:

$$[A_2A_3(-A_4)]^{-1/2} \arcsin\{[2A_2(-A_4)u^+ - (A_2 + A_4)]/[(A_2 + A_4)^2 + 4(A_2)(-A_4)]^{1/2}\} - \tfrac{1}{2}\ln[A_3(1 + A_4u^+)(1 + A_2u^+)] + (A_2/a_1)[A_3(1 + A_4u^+)(1 + A_2u^+)]^{-1/2} = \int(1/L^+)dy^+ + C_2 = F_{II}(u^+) \quad (26)$$

In these expressions, C_1 and C_2 are constants of integration. The constant C_1 is evaluated by letting $u^+ \to 0$ in the terms on the left-hand side of Eq. (25). Then the constant C_2 is evaluated by matching the left-hand side of each of Eqs. (25) and (26) at the flame front.

These functions have been utilized in correlating the experimental results of Wooldridge and Muzzy[6] and Jones.[7] In these separate studies, subsonic, low-turbulence wind tunnels were employed to obtain turbulent boundary layers into which mass was injected and combustion occurred. The test sections of these wind tunnels were 8 ft in length with the last 2 ft of the top surfaces fitted with porous plates. Dilute mixtures of hydrogen and nitrogen were injected through the porous plates into the turbulent boundary layers. The mixtures were ignited and combustion maintained in each of the boundary layers.

In the experiments conducted by Wooldridge and Muzzy, profiles of concentration, temperature, and dynamic pressure were taken at the trailing edge of the porous plate region. Three widely different mass injection rates were employed. The experimental conditions for these profiles are indicated in Table 1. In the experiments conducted by Jones, profiles of temperature and dynamic pressure were taken at three different axial stations with the experimental conditions also presented in Table 1. In these latter experiments, the mass injection rate was held constant. In all of these experiments, the axial pressure gradient was approximately zero.

The velocity profiles deduced from the experimental dynamic pressure profiles have been utilized in the left-hand side of each of Eqs. (25) and (26) and the results plotted against $\log y^+$ in Fig. 1. It becomes apparent from the results presented that there is an inner region of the boundary layer inside the flame front over which the dissipation length L^+ is proportional to y^+ or in which $L^+ = Ky^+$. This inner region extends to $y = 0.09$ in. at the low blowing rates and increases to a distance $y = 0.20$ in. for the larger blowing rates. It should also be noted that K seems to be dependent upon the terms A_1 and A_2 with the value of K increasing considerably above the value of 0.4 which is obtained from constant density boundary layers. For example, at $F = 2.34 \times 10^{-3}$, $K = 0.95$ while at $F = 7.56 \times 10^{-3}$, K has increased to approximately 3.

From the results presented in Fig. 1, we may conclude that in the analysis of subsonic turbulent boundary layers with large normal variations in density, it appears feasible to separate the density variation from the variation of the turbulent characteristics of the flow and treat each independently of the other. It should also be noted that the analytical results are presented in a form which should allow verification of the approach by statistical means, especially through the use of cooled constant temperature film probes. These types of measurements could yield a direct indication of the behavior of such parameters as the dissipation length L^+.

Finally, the constant of integration C_1 may be approximated by letting u^+ go to zero, yielding the result

$$C_1 = [2/(A_1A_2)^{1/2}] \ln[(A_1)^{1/2} + (A_2)^{1/2}] + A_2/a_1$$

Inclusion of this constant in Eqs. (25) and (26) yields the results presented in Fig. 2 where 4 of the 6 curves have col-

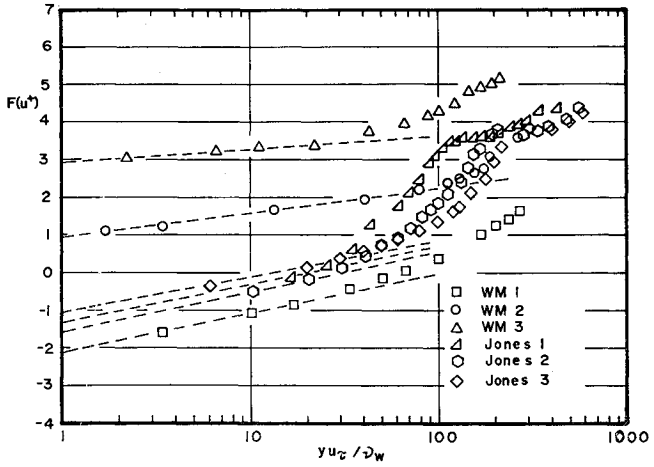

Fig. 1 Experimental nondimensional velocity function $F(u+)$ plotted vs nondimensionalized distance for the subsonic turbulent boundary layer with mass addition and combustion.

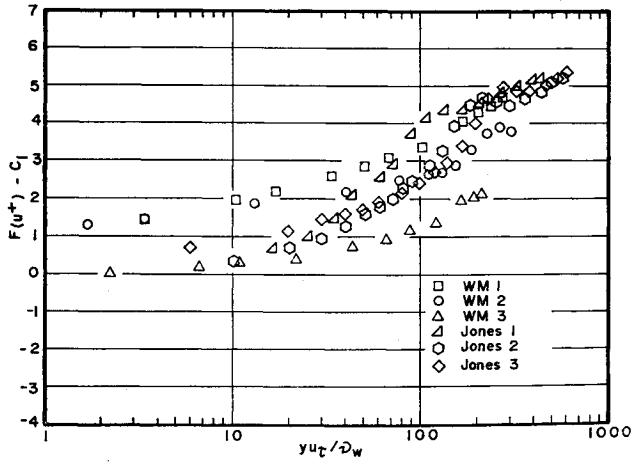

Fig. 2 Experimental nondimensional velocity function including the constant of integration $F(u+) - C_1$ plotted vs nondimensionalized distance.

lapsed approximately into a common band in the inner region ($y^+ < 40$). An explanation for the deviation of the other two curves has not been formulated.

References

[1] Townsend, A. A., "Equilibrium Layers and Wall Turbulences," *Journal of Fluid Mechanics*, Vol. 11, Pt. 1, Aug. 1961, pp. 97–120.

[2] Bradshaw, P., Ferriss, D. H., and Atwell, N. P., "Calculation of Boundary-Layer Development Using the Turbulent Energy Equation," *Journal of Fluid Mechanics*, Vol. 28, Pt. 3, May 1967, pp. 593–616.

[3] Bradshaw, P., "The Turbulence Structure of Equilibrium Boundary Layers," *Journal of Fluid Mechanics*, Vol. 29, Pt. 4, Sept. 1967, pp. 625–645.

[4] Bradshaw, P. and Ferriss, D. H., "Calculation of Boundary Layer Development Using the Turbulent Energy Equation; IV: Heat Transfer with Small Temperature Differences," Aero Rept. 1271, 1968, National Physics Lab.

[5] Chen, T. N. and Toong, T. Y., "Laminar Boundary-Layer Wedge Flows with Evaporation and Combustion," AIAA Paper 63-449, Palm Beach, Fla., 1963.

[6] Wooldridge, C. E. and Muzzy, R. J., "Measurements in a Combusting Turbulent Boundary Layer with Porous Wall Injection," *Tenth Symposium (International) on Combustion*, the Combustion Institute, Pittsburgh, Pa., 1965.

[7] Jones, J. W., "A Turbulent Boundary Layer with Mass Addition, Combustion, and Pressure Gradient," Ph.D. dissertation, Department of Mechanical Engineering, Univ. of Utah (to be published).

Integral Method for Internal Hypersonic Flows

LEVON M. MINASSIAN*
Canadair Ltd., Montreal, Canada

Nomenclature

e = specific internal energy
M = Mach number
p = static pressure
U = freestream velocity
u = axial velocity in the shock layer
v = lateral velocity ($\perp$ to freestream) in the shock layer
x,y = nondimensional Cartesian coordinates in terms of leading-edge radius y_0
ρ = density
γ = ratio of specific heats = 1.4
ϵ = density ratio across shock, ρ_∞/ρ_s
σ = angle between shock wave and freestream

Superscripts

$'$ = first derivative with respect to x
$''$ = second derivative with respect to x
$'''$ = third derivative with respect to x

Subscripts

0 = condition at the leading edge
1 = condition at a general point
s = condition at the shock
∞ = condition at freestream
b = condition at the body

Received November 17, 1969; revision received February 26, 1970. The author expresses his gratitude to S. Mölder of McGill University for making available the results of the method of characteristics.

* Research Engineer, Technology Development—Aerodynamics.

Introduction

THE Note presents the formulation and the numerical results of an integral method, thin-shock-layer analysis. The solution is obtained by integration of a single ordinary differential equation, which determines both the shock shape and surface pressure.

Formulation of the Problem

The integral conservation equations across the shock layer may be expressed for internal axisymmetric flows between two axial stations x_0 and x_1.

Continuity:

$$\rho_\infty U(y_0^2 - y_{s_1}^2)/2 = \int_{y_{s_1}}^{y_b} \rho u y dy \tag{1}$$

Axial Momentum:

$$(p_\infty + \rho_\infty U^2)(y_0^2 - y_{s_1}^2)/2 = \int_{y_{s_1}}^{y_{b_1}} (p + \rho u^2) y dy - \int_{y_0}^{y_{b_1}} p_b y_b dy_b \tag{2}$$

Lateral Momentum:

$$\int_{y_{s_1}}^{y_{b_1}} \rho u v y dy = \int_{x_0}^{x_1} (p_\infty - p_s) y_s dx \tag{3}$$

Energy:

$$\rho_\infty U[e_\infty + (p_\infty/\rho_\infty) + U^2/2](y_0^2 - y_{s_1}^2)/2 = \int_{y_{s_1}}^{y_{b_1}} \rho u[e + (p/\rho) + (u^2 + v^2)/2] y dy \tag{4}$$

The concept of thin-shock-layer theory stipulates constancy of flow variables across the shock layer between shock and body. The pressure and the lateral velocity v are thus assumed to vary only in the axial direction. Following Chernyi[1,2] the constant pressure across the layer is assumed to be equal to its wall value p_b. The constant lateral velocity is taken equal to its value behind the shock

$$v = v_s = U y_s'(1 - \epsilon) = [2U y_s'/(\gamma + 1)][1 - 1/(M_\infty^2 y_s'^2)] \tag{5}$$

In addition, u is assumed to be equal to U. This approach is fully justified in the limit as $\epsilon \to 0$. Chernyi claims reasonably accurate results with values as high as 0.3.

The above assumptions, made by Hayes and Probstein[3] in their analysis for external flows, confine the problem to slender bodies. Two approaches will be considered to overcome this restriction.

In the first approach, Eq. (5) is determined from the continuity relationship across an oblique shock, assuming $\sin^2\sigma = y_s'^2$. This assumption underestimates the magnitude of the first and second derivatives of y_s, thus resulting in a thinner shock layer; v_s in Eq. (5) therefore is underestimated. The assumption $u \approx U$ overestimates u. For large M_∞ and inlet angles, the lowering of values of v_s is the stronger of the two effects and hence the pressure in the shock layer is expected to be overestimated. The exact form of Eq. (5) is:

$$v_s/U = 2y_s'[1 - (1 + y_s'^2)/(M_\infty^2 y_s'^2)]/[(\gamma + 1) \times (1 + y_s'^2)] \tag{6}$$

Substitute Eq. (6) in the exact form of u/U from two-dimensional oblique relations to obtain

$$u/U = 2\{[(\gamma + 1)/2] + (1/M_\infty^2) - y_s'^2/(1 + y_s'^2)\}/(\gamma + 1) \tag{7}$$

With the aid of Eq. (1) and assuming constancy of flow variables across the shock layer, Eq. (3) may be differentiated with respect to x resulting in

$$p_b/(\rho_\infty U^2) = [1/(M_\infty^2)] + (y_s' v_s/U) + (y_0^2 - y_s^2)(v_s'/U)/(2y_s) \tag{8}$$